

Обзор ArXiv/astro-ph,  
9-13 марта 2020 года

От Сильченко О.К.

# ArXiv: 2003.03368

## The Grand Twirl: The Epoch of Rapid Assembly of Extended and Quiescent Discs

Michael Kretschmer<sup>1\*</sup>, Oscar Agertz<sup>2</sup> and Romain Teyssier<sup>1</sup>

<sup>1</sup>*Institute for Computational Science, University of Zurich, Winterthurerstrasse 190, CH-8057 Zurich, Switzerland*

<sup>2</sup>*Lund Observatory, Department of Astronomy and Theoretical Physics, Lund University, Box 43, SE-221 00 Lund, Sweden*

Accepted XXX. Received YYY; in original form ZZZ

### ABSTRACT

Galactic outflows driven by stellar feedback are crucial for explaining the inefficiency of galaxy formation. Although strong feedback can promote the formation of galactic discs by limiting star formation at early times and removing low angular momentum gas, it is not understood how the same feedback can result in diverse objects such as elliptical galaxies or razor thin spiral galaxies. In this work, we investigate this problem using cosmological zoom-in simulations of two galaxies forming within  $10^{12} M_{\odot}$  halos with almost identical mass accretion histories. At  $z > 1.5$ , the two galaxies feature a surface density of star formation  $\Sigma_{\text{SFR}} \approx 10 M_{\odot} \text{ yr}^{-1} \text{ kpc}^{-2}$ , leading to strong outflows. After the last starburst episode, both galaxies feature a dramatic gaseous disc growth from 1 kpc to 5 kpc during 1 Gyr, a decisive epoch we dub “the Grand Twirl”.

# Большое завихрение!

# Изысканные модели: LCDM (RAMSES)+ физика SF

dark matter particle mass of  $m_{\text{dm}} = 2.0 \times 10^5 M_{\odot}$  and an initial baryonic mass resolution of  $m_{\text{bar}} = 2.9 \times 10^4 M_{\odot}$ .

We subsequently carried out our final simulations including gas and galaxy formation physics, as summarized below. The maximum resolution was set to  $\ell_{\text{max}} = 19$  at  $z = 0$ , with refinement levels progressively released to enforce a quasi-constant physical resolution, where the smallest cells have sizes  $\Delta x_{\text{min}} = 55 \text{pc}$ . The adopted refinement criterion is the traditional quasi-Lagrangian approach, namely cells are individually refined when more than 8 dark matter particles are present or when the total baryonic mass (gas and stars) exceeds  $8 \times m_{\text{bar}}$ . Only the Lagrangian volume corresponding to twice the final virial radius of the halo was adaptively refined, the rest of the box being kept at a fixed, coarser resolution to provide the proper tidal field.

We intentionally picked halos without any major mergers at  $z < 1$  and with overall similar mass accretion histories. The halos feature a strong merger-induced starburst at  $z = 1.4$  and  $z = 2.0$  respectively, followed by quiescent accretions history until  $z = 0$ . The final dark matter halo spin parameters, as defined in [Bullock et al. \(2001\)](#), are very similar for both halos, namely  $\lambda = 0.015$  and  $\lambda = 0.014$ . This fact

For our star formation recipe, we adopt a traditional Schmidt law, for which the star formation rate density is given by

$$\dot{\rho}_{\star} = \epsilon_{\text{ff}} \frac{\rho}{t_{\text{ff}}} \quad (1)$$

where  $\rho$  is the density of the gas,  $t_{\text{ff}} = \sqrt{3\pi/(32G\rho)}$  is its free-fall time and  $\epsilon_{\text{ff}}$  is the star formation efficiency per free-fall

in a turbulent medium, like the interstellar medium (ISM), the gas density distribution is well described by a log-normal probability distribution function (PDF):

$$p(s) = \frac{1}{\sqrt{2\pi\sigma_s^2}} \exp\left(-\frac{(s-\bar{s})^2}{2\sigma_s^2}\right), \quad (2)$$

where  $s = \ln \rho/\rho_0$ ,  $\sigma_s$  is the variance of  $s$ ,  $\rho$  is the gas density and  $\rho_0$  the mean density.

$$\begin{aligned} \epsilon_{\text{ff}} &= \frac{\epsilon}{\phi_t} \int_{s_{\text{crit}}}^{\infty} \frac{t_{\text{ff}}(\rho_0)}{t_{\text{ff}}(\rho)} \frac{\rho}{\rho_0} p(s) ds \\ &= \frac{\epsilon}{2\phi_t} \exp\left(\frac{3}{8}\sigma_s^2\right) \left[1 + \text{erf}\left(\frac{\sigma_s^2 - s_{\text{crit}}}{\sqrt{2}\sigma_s}\right)\right]. \end{aligned} \quad (3)$$

We compute  $s_{\text{crit}}$  using the model of [Krumholz & McKee \(2005\)](#) for which  $s_{\text{crit}}$  is estimated by requiring the virial parameter of the gas to be less than 1. We slightly modify the original model to account for subsonic and transonic cases such that for  $\mathcal{M} < 1$  we require that the entire computational cell becomes gravitational unstable. With this, we can use the modified model for both regime  $\mathcal{M} \leq 1$  and  $\mathcal{M} \geq 1$ . The obtained critical density for star formation is

$$s_{\text{crit}} = \ln \left[ \alpha_{\text{vir}} \left( 1 + \frac{2\mathcal{M}^4}{1 + \mathcal{M}^2} \right) \right], \quad (4)$$

where

$$\alpha_{\text{vir}} = \frac{5\sigma^2}{3G\rho\Delta x^2} \quad (5)$$

is the local virial number which can be interpreted as an estimator for the local stability,  $\Delta x$  is the cell size and  $\sigma$  is the turbulent 1D velocity dispersion which is computed by the subgrid scale (SGS) turbulent energy model (see [Schmidt](#)

# «Два зверя благородных...»

газ!

все!

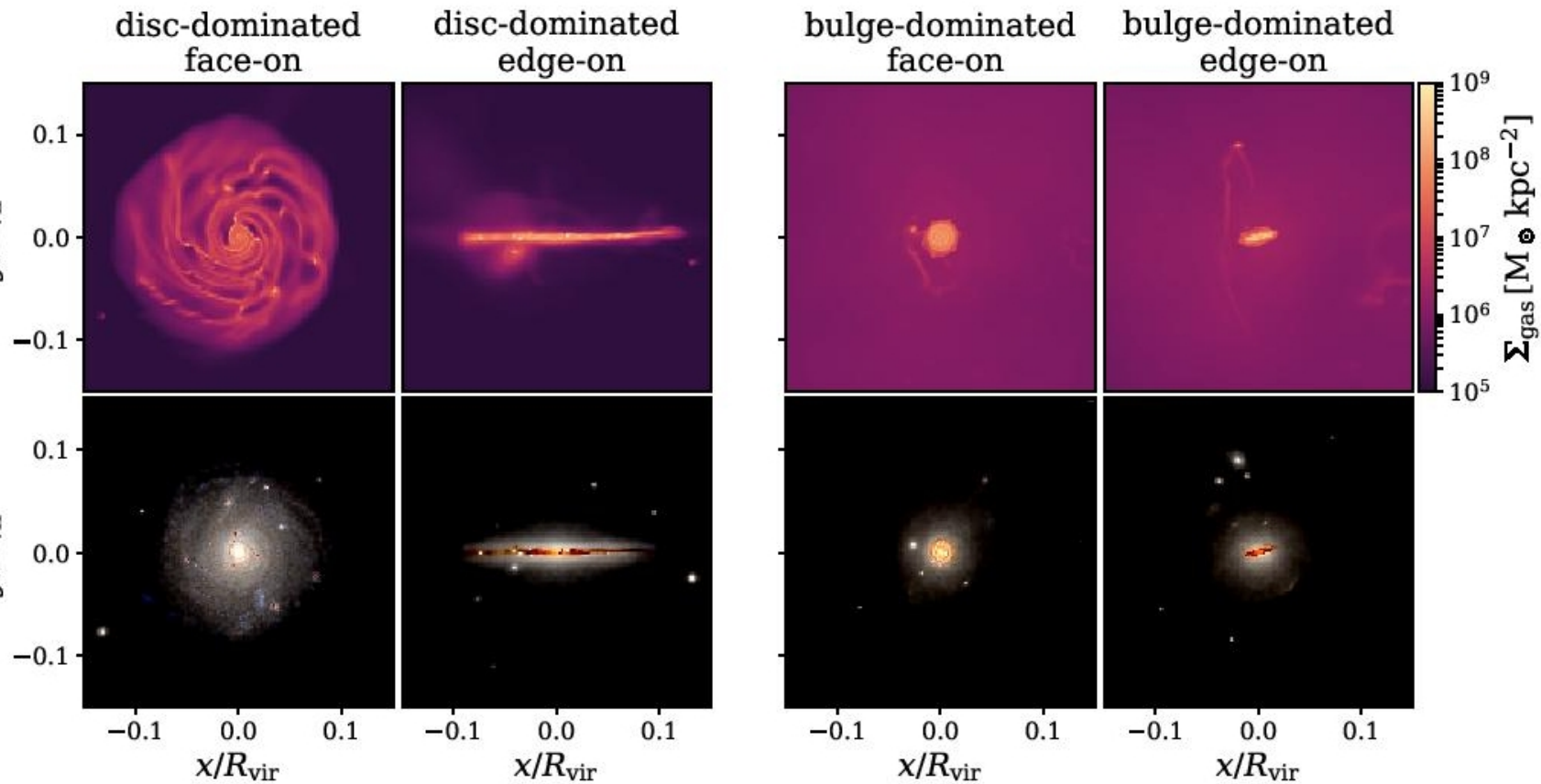


**Figure 1.** Projected maps of the two galaxies at  $z = 0$ . Left two columns are the disc-dominated galaxy face-on and edge-on. Right two columns are the bulge-dominated galaxy face-on and edge-on. The top row shows the gas surface density and the bottom row shows true colour images with dust absorption allowing us to render both stars and gas.

# Их истории (всего разного)

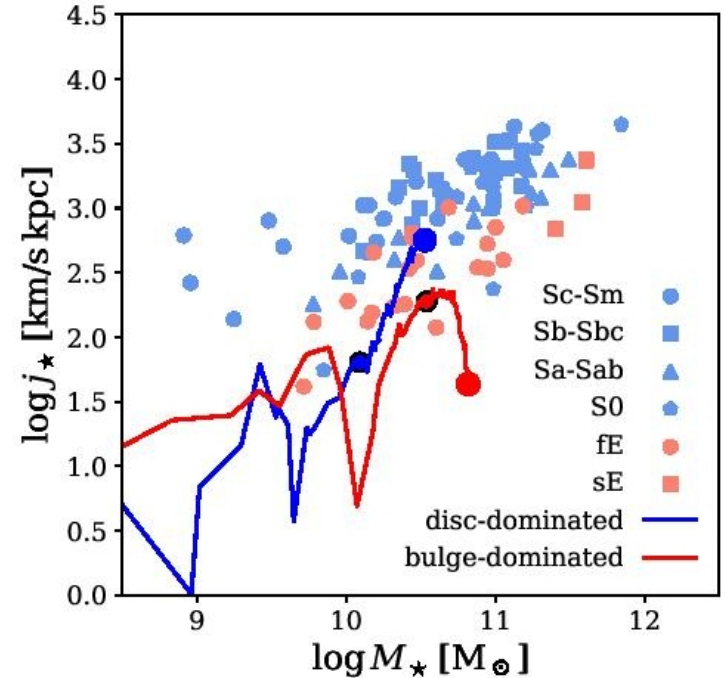
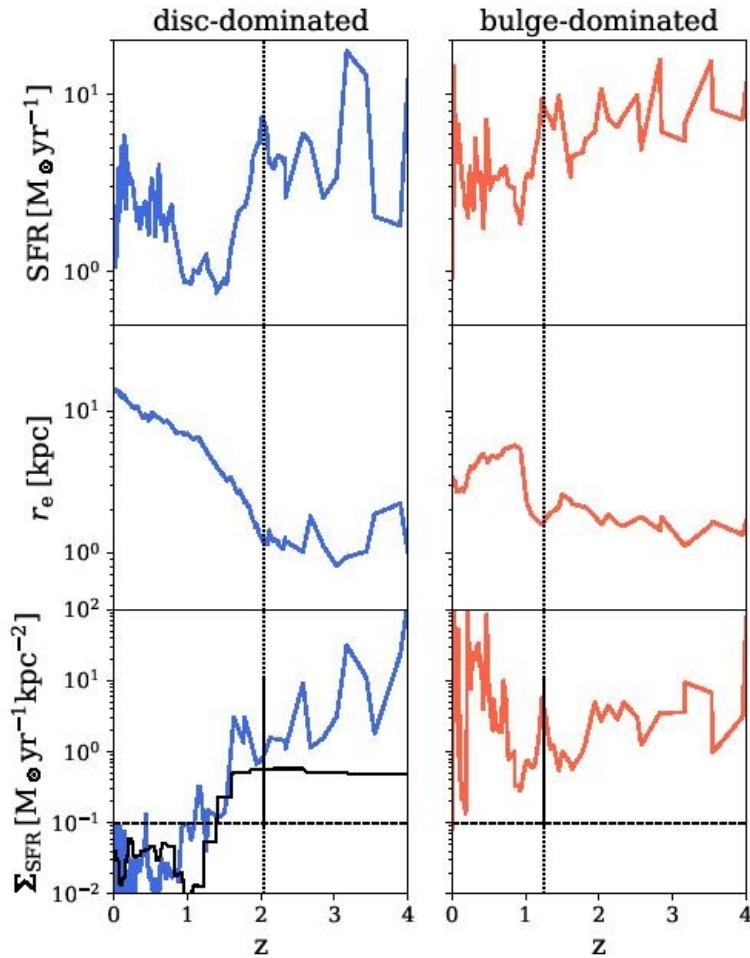


**Figure 3.** Evolution of the specific angular momentum of the stars for the two galaxies as a function of their stellar mass. Blue is the galaxy that will end up as a disc-dominated galaxy at  $z = 0$  and red is the bulge-dominated. The small circle in the same color of the line is the moment of the last starburst. The big circle is the point at  $z = 0$ . Data points are taken from [Fall & Romanowsky \(2013\)](#), where circles are ellipticals and others are spirals.

# Моменты (карты и статистика)

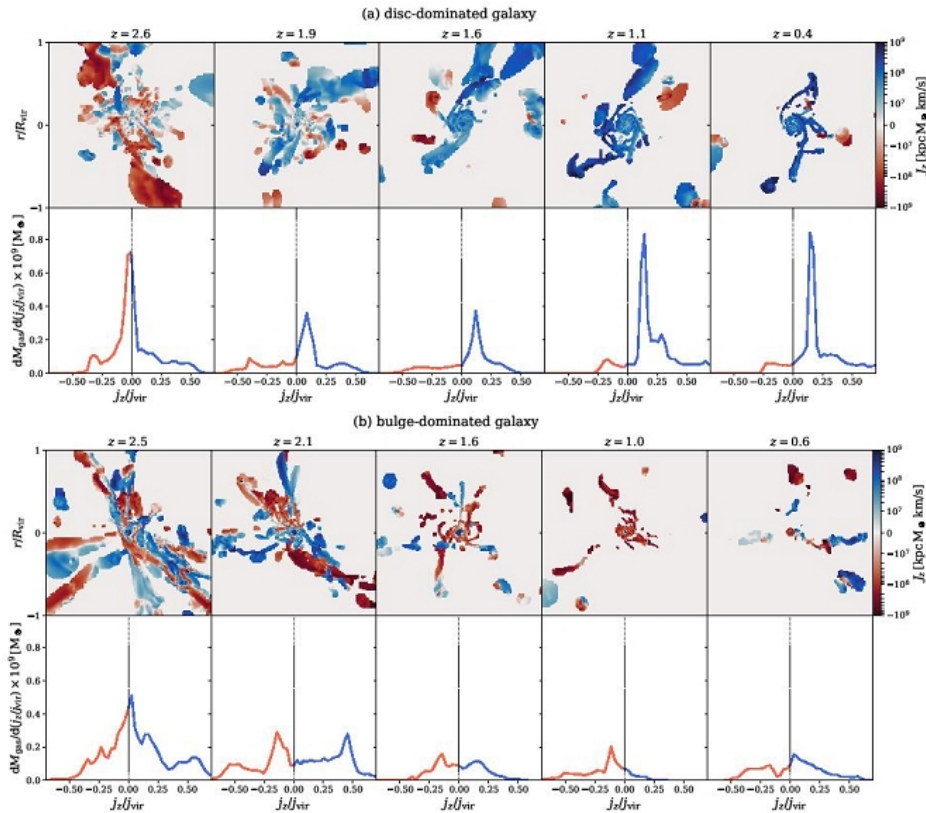


**Figure 4.** Evolution of the mass-weighted cold gas angular momentum (AM) in the virial radius of the disc-dominated galaxy (a) and bulge-dominated galaxy (b). Plots are done at  $z \sim 2.5, 2.0, 1.5, 1.0, 0.5$ . **Top rows:** Mass-weighted map of cold gas angular momentum in the virial radius. Colours indicate the sign of the angular momentum where red corresponds to counter-rotating gas and blue co-rotating. For the disc-dominated galaxy, most of the cold gas is joining the disc constructively. An extended disc of cold gas is seen. In contrast, for the bulge-dominated galaxy, most of the cold gas is counter-rotating with respect to the disc. This causes the net disc to shrink. **Bottom rows:** Mass-weighted distribution of specific angular momentum of infalling cold gas measured between  $< r/R_{vir} < 1.0$  normalised by the specific virial AM of a given snapshot.  $j_z$  is measured with respect to the disc AM inside  $0.1R_{vir}$ . For disc-dominated galaxy, most infalling cold gas has positive  $j_z/j_{vir}$  resulting in constructive AM. For the bulge-dominated galaxy, the distribution shows positive and negative contributions where sometimes the destructive part is dominating. Infalling cold gas therefore adds destructive AM to the disc.

газ

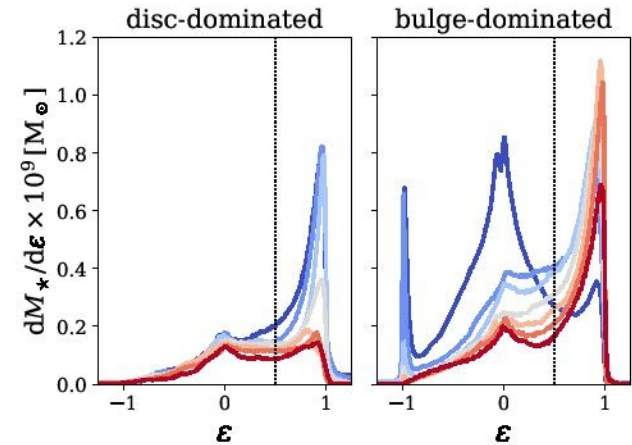


**Figure 5.** Evolution of the distribution of circularity  $\epsilon$ . Shown is the stellar mass per bin. The first snapshot in red coincides with the last star-burst: The disc-dominated galaxy (left) has similar mass in the bulge and disc-components. The bulge-dominated has a more dominant disc component. Time evolution is shown as transitions to bluer colors in steps of  $\approx 1.5$  Gyrs until the final snapshot at  $z = 0$  in dark blue. Here the disc-dominated has a dominant disc-component and a small bulge. The bulge-dominated has a large bulge-component and counter-rotating stars.

звезды

# ArXiv: 2003.04935

## Cosmic Discordance: Planck and luminosity distance data exclude LCDM.

Eleonora Di Valentino,<sup>1,\*</sup> Alessandro Melchiorri,<sup>2,†</sup> and Joseph Silk<sup>3,4,5,‡</sup>

<sup>1</sup>*Jodrell Bank Center for Astrophysics, School of Physics and Astronomy,  
University of Manchester, Oxford Road, Manchester, M13 9PL, UK*

<sup>2</sup>*Physics Department and INFN, Università di Roma “La Sapienza”, Ple Aldo Moro 2, 00185, Rome, Italy*

<sup>3</sup>*Institut d’Astrophysique de Paris (UMR7095: CNRS & UPMC- Sorbonne Universities), F-75014, Paris, France*

<sup>4</sup>*Department of Physics and Astronomy, The Johns Hopkins University Homewood Campus, Baltimore, MD 21218, USA*

<sup>5</sup>*BIPAC, Department of Physics, University of Oxford, Keble Road, Oxford OX1 3RH, UK*

(Dated: March 12, 2020)

We show that a combined analysis of CMB anisotropy power spectra obtained by the Planck satellite and luminosity distance data simultaneously excludes a flat universe and a cosmological constant at 99% C.L.. These results hold separately when combining Planck with three different datasets: the two determinations of the Hubble constant from Riess et al. 2019 and Freedman et al. 2020, and the Pantheon catalog of high redshift supernovae type-Ia. We conclude that either LCDM needs to be replaced by a drastically different model, or else there are significant but still undetected systematics. Our result calls for new observations and stimulates the investigation of alternative theoretical models and solutions.

# Предлагается модификация модели – дополнительные параметры:

- Кривизна пространства  $\Omega_k$
- Эволюция наклона и амплитуды спектра возмущений
- Уравнение состояния темной энергии:  
 $P = -\omega \rho$
- Суммарная масса нейтрино ( $\gg 0.06$  эВ)



# По каким данным «натягивают» модель:

- Чистый Planck2018
- Planck+BAO
- Planck+Riess19 (SNIa,  $H_0 = 74$ )
- Planck+Freedman20 (вершина ветви красных гигантов,  $H_0 = 69$  с копеечкой)
- Planck+Pantheon (альтернативный набор сверхновых SNIa)

# Решит ли проблему введение дополнительных параметров?

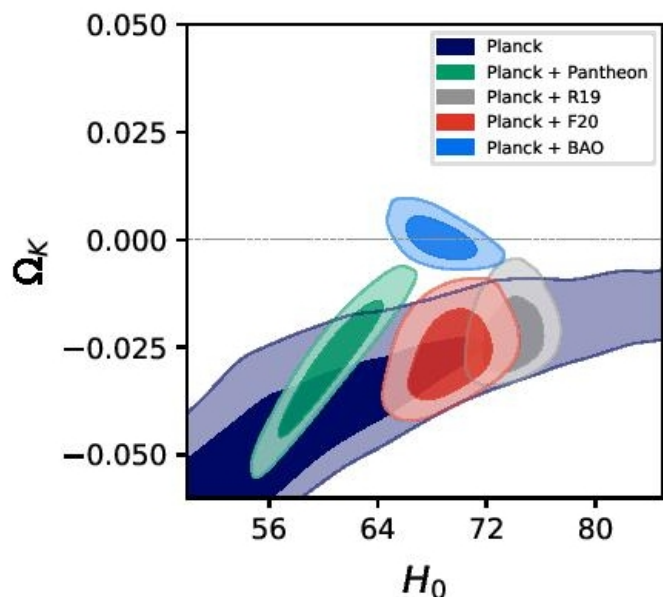


Figure 1. **Cosmic Discordance.** Constraints at the 68% and 95% C.L. on the  $\Omega_k$  vs  $H_0$  plane for the Planck, Planck+R19, Planck+F20, Planck+BAO, and Planck+Pantheon datasets. A 10 parameters model,  $\Lambda\text{CDM}+w+\Omega_k+\alpha_S+\Sigma m_\nu$ , is assumed in the analysis.

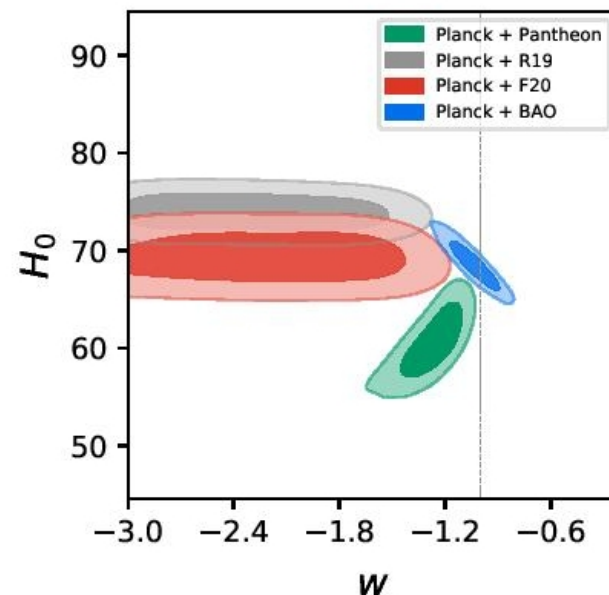


Figure 2. **Cosmic Discordance.** Constraints at the 68% and 95% C.L. on the  $w$  vs  $H_0$  plane for the Planck+R19, Planck+F20, Planck+BAO, and Planck+Pantheon datasets. A 10 parameter model,  $\Lambda\text{CDM}+w+\Omega_k+\alpha_S+\Sigma m_\nu$ , is assumed in the analysis.

# Результаты для 12 параметров по 5 комбинациям данных

Parameters	Planck	Planck +R19	Planck +F20	Planck +BAO	Planck + Pantheon
$\Omega_b h^2$	$0.02253 \pm 0.00019$	$0.02253^{+0.00020}_{-0.00016}$	$0.02255^{+0.00019}_{-0.00017}$	$0.02243 \pm 0.00016$	$0.02255 \pm 0.00018$
$\Omega_c h^2$	$0.1183 \pm 0.0016$	$0.1187^{+0.0015}_{-0.0018}$	$0.1184 \pm 0.0015$	$0.1198 \pm 0.0014$	$0.1186 \pm 0.0015$
$100\theta_{MC}$	$1.04099 \pm 0.00035$	$1.04103^{+0.00034}_{-0.00031}$	$1.04105 \pm 0.00034$	$1.04095 \pm 0.00032$	$1.04107 \pm 0.00034$
$\tau$	$0.0473 \pm 0.0083$	$0.052^{+0.009}_{-0.011}$	$0.0491 \pm 0.0079$	$0.0563 \pm 0.0081$	$0.0506 \pm 0.0082$
$\Sigma m_\nu$ [eV]	$0.43^{+0.16}_{-0.37}$	$< 0.513$	$0.28^{+0.11}_{-0.23}$	$< 0.194$	$< 0.420$
$w$	$-1.6^{+1.0}_{-0.8}$	$-2.11^{+0.35}_{-0.77}$	$-2.14 \pm 0.46$	$-1.038^{+0.098}_{-0.088}$	$-1.27^{+0.14}_{-0.09}$
$\Omega_k$	$-0.074^{+0.058}_{-0.025}$	$-0.0192^{+0.0036}_{-0.0099}$	$-0.0263^{+0.0060}_{-0.0077}$	$0.0003^{+0.0027}_{-0.0037}$	$-0.029^{+0.011}_{-0.010}$
$\ln(10^{10} A_s)$	$3.025 \pm 0.018$	$3.037^{+0.016}_{-0.026}$	$3.030 \pm 0.017$	$3.049 \pm 0.017$	$3.034 \pm 0.017$
$n_s$	$0.9689 \pm 0.0054$	$0.9686^{+0.0056}_{-0.0050}$	$0.9693 \pm 0.0051$	$0.9648 \pm 0.0048$	$0.9685 \pm 0.0051$
$\alpha_S$	$-0.0005 \pm 0.0067$	$-0.0012 \pm 0.0066$	$-0.0010 \pm 0.0068$	$-0.0054 \pm 0.0068$	$-0.0023 \pm 0.0065$
$H_0$ [km/s/Mpc]	$53^{+6}_{-16}$	$73.8 \pm 1.4$	$69.3 \pm 2.0$	$68.6^{+1.5}_{-1.8}$	$60.5 \pm 2.5$
$\sigma_8$	$0.74^{+0.08}_{-0.16}$	$0.932 \pm 0.040$	$0.900 \pm 0.039$	$0.821 \pm 0.027$	$0.812^{+0.031}_{-0.018}$
$S_8$	$0.989^{+0.095}_{-0.063}$	$0.874 \pm 0.032$	$0.900^{+0.034}_{-0.031}$	$0.826 \pm 0.016$	$0.927 \pm 0.037$
$Age$ [Gyr]	$16.10^{+0.92}_{-0.80}$	$14.90^{+0.72}_{-0.32}$	$15.22^{+0.054}_{-0.038}$	$13.77 \pm 0.10$	$14.98 \pm 0.39$
$\Omega_m$	$0.61^{+0.21}_{-0.34}$	$0.264^{+0.010}_{-0.013}$	$0.300^{+0.017}_{-0.020}$	$0.305 \pm 0.016$	$0.393^{+0.030}_{-0.036}$
$\Delta\chi^2_{best\,fit}$	0.0	0.62	0.88	14.77	1037.82

Table I. Constraints at 68% CL errors on the cosmological parameters in case of the 12 parameters model using different combinations of the datasets. The quoted upper limits are at 95% CL. In the bottom line we quote the difference in the best-fit  $\chi^2$  values with respect to the Planck data alone result.